

## OUTFLOW-DOMINATED EMISSION FROM THE QUIESCENT MASSIVE BLACK HOLES IN NGC 4621 AND NGC 4697

J. M. WRABEL,<sup>1</sup> Y. TERASHIMA,<sup>2</sup> AND L. C. HO<sup>3</sup>

*To appear in the Astrophysical Journal*

### ABSTRACT

The nearby elliptical galaxies NGC 4621 and NGC 4697 each host a supermassive black hole with  $M_{\bullet} > 10^8 M_{\odot}$ . Analysis of archival *Chandra* data and new NRAO Very Large Array data shows that each galaxy contains a low-luminosity active galactic nucleus (LLAGN), identified as a faint, hard X-ray source that is astrometrically coincident with a faint 8.5-GHz source. The latter has a diameter less than  $0.3''$  (26 pc for NGC 4621, 17 pc for NGC 4697). The black holes energizing these LLAGNs have Eddington ratios  $L(2-10 \text{ keV})/L(\text{Edd}) \sim 10^{-9}$ , placing them in the so-called quiescent regime. The emission from these quiescent black holes is radio-loud, with  $\log R_X = \log \nu L_{\nu}(8.5 \text{ GHz})/L(2-10 \text{ keV}) \sim -2$ , suggesting the presence of a radio outflow. Also, application of the radio-X-ray-mass relation from Yuan & Cui for quiescent black holes predicts the observed radio luminosities  $\nu L_{\nu}(8.5 \text{ GHz})$  to within a factor of a few. Significantly, that relation invokes X-ray emission from the outflow rather than from an accretion flow. The faint, but detectable, emission from these two massive black holes is therefore consistent with being outflow-dominated. Observational tests of this finding are suggested.

*Subject headings:* galaxies: active — galaxies: individual (NGC 4621, NGC 4697) — galaxies: nuclei — radio continuum: galaxies — X-rays: galaxies

### 1. MOTIVATION

Dynamical studies have established that supermassive black holes, with masses  $M_{\bullet} \sim 10^6 - 10^9 M_{\odot}$ , occur in the nuclei of most nearby galaxies with stellar bulges (e.g., Kormendy 2004). Yet few of these massive black holes are observed as luminous active galactic nuclei (AGNs). Rather, the Palomar spectroscopic survey by Ho et al. (1997) showed that the majority have either no AGN signatures or only the weak AGN signatures that define them as low-luminosity AGNs (LLAGNs;  $L(H\alpha) \leq 10^{40} \text{ ergs s}^{-1}$ ). Also, *Chandra* surveys of selected Palomar LLAGNs (Ho et al. 2001; Terashima & Wilson 2003) commonly find X-ray nuclei with  $L(2-10 \text{ keV}) = 10^{38} - 10^{42} \text{ ergs s}^{-1}$ , leading to  $L(2-10 \text{ keV}) < 10^{42} \text{ ergs s}^{-1}$  as an X-ray definition of a LLAGN. For the black hole masses involved, such  $H\alpha$  and X-ray luminosities are highly sub-Eddington, that is, much less than the Eddington luminosity  $L(\text{Edd}) = 1.3 \times 10^{38} (M_{\bullet}/M_{\odot}) \text{ ergs s}^{-1}$ . Understanding the radiative quiescence of these massive black holes has important implications for accretion physics, fuelling and feedback mechanisms, and black-hole growth over cosmic time (Ho 2004; Pellegrini 2005).

Early theoretical models for weakly-radiating massive black holes invoked radiatively-inefficient inflows (e.g., Narayan et al. 1995), jets/outflows (e.g., Falcke & Markoff 2000), and combinations of the two (e.g., Yuan et al. 2000a). The models predicted that continuum emission could emerge in the radio and hard X-ray regions. For LLAGNs, these frequency re-

gions offer strong tests of the models because they benefit from high contrast against the stellar emission, little or no obscuration, and subarcsecond angular resolution and astrometry. Significantly, a study of Palomar LLAGNs using *Chandra*, the Very Large Array (VLA), and the Very Long Baseline Array (VLBA), found that the majority are radio loud, defined as  $\log R_X = \log \nu L_{\nu}(5 \text{ GHz})/L(2-10 \text{ keV}) = -4.5$  or higher (Terashima & Wilson 2003). Since LLAGNs may possess radiatively-inefficient accretion flows (e.g., Yuan et al. 2000b) and radio continuum emission is outflow-dominated (e.g., Falcke & Biermann 1999; Nagar et al. 2005), this suggests that such accretion flows can produce outflows more efficiently than standard geometrically thin accretion disks (Livio et al. 1999; Meier 2001). Moreover, such radio continuum outflows might have sufficiently stable “astrometric footprints” to constrain the proper motions of their galaxy hosts in the extragalactic frame (e.g., Bietenholz et al. 2000), especially for galaxy hosts which lack interstellar water masers.

Building upon the work by Terashima & Wilson (2003), Ho et al. (2003b) and Terashima et al. (2005) searched in the radio and X-ray regions for LLAGN signatures from the weakest accretors, namely nearby Palomar nuclei showing no or very weak  $H\alpha$  (Ho et al. 2003a). Those targets were mainly disk galaxies and the new *Chandra* detections of them correspond to X-ray nuclei with  $L(2-10 \text{ keV}) < 10^{38} \text{ ergs s}^{-1}$  (Ho et al. 2003b; Terashima et al. 2005). With their typical  $M_{\bullet} < 10^8 M_{\odot}$ , these accretors are feeble emitters with Eddington ratios  $L(2-10 \text{ keV})/L(\text{Edd}) < 10^{-7}$ . Still, Terashima et al. (2005) obtained VLA detections of radio nuclei at the levels predicted from the radio-loudness relation (Terashima & Wilson 2003), proving that the trait of radio loudness holds below  $L(2-10 \text{ keV}) = 10^{38} \text{ ergs s}^{-1}$  and continuing to emphasize the potential importance of radio outflows from these modest-mass

<sup>1</sup> National Radio Astronomy Observatory, P.O. Box O, Socorro, NM 87801; jwrobel@nrao.edu

<sup>2</sup> Department of Physics, Faculty of Science, Ehime University, Matsuyama 790-8577, Japan; terashima@astro.phys.sci.ehime-u.ac.jp

<sup>3</sup> The Observatories of the Carnegie Institution of Washington, 813 Santa Barbara Street, Pasadena, CA 91101; lho@ociw.edu

black holes.

Encouraged by these X-ray/radio trends, a next step is to search for continuum signatures of LLAGNs in nearby elliptical galaxies, with their typically higher  $M_{\bullet}$ . Archival and published data from *Chandra* and the VLA are used in § 2 to identify two candidate LLAGNs in nearby elliptical galaxies. New high-resolution observations of these candidates with the VLA<sup>4</sup> (Thompson et al. 1980) are reported in § 3. The implications of the new VLA imaging are explored in § 4 regarding the astrometry, and in § 5 regarding the photometry. § 6 closes with a summary of this work and suggestions for future directions.

## 2. PRIOR DATA

A Palomar elliptical galaxy NGC 4621 and a southern elliptical galaxy NGC 4697 were selected. NGC 4621 is an absorption-line nucleus with an H $\alpha$  upper limit from Ho et al. (2003a). NGC 4697 has modest LINER characteristics (Pinkney et al. 2005; J. Pinkney, priv. comm.). For each galaxy, Table 1 lists its surface-brightness-fluctuation distance and scale, as well the mass and Eddington luminosity of its black hole. Table 2 gives the centroid positions of the galaxies from NED/2MASS.

### 2.1. VLA

At the NED/2MASS centroid positions, the galaxies are neither confused nor detected at 1.4 GHz, and thus are less than 2.5 mJy at 45'' resolution (Condon et al. 1998) and less than 1 mJy at 5'' resolution (White et al. 1997). From VLA data at 5 GHz and 5'' resolution, NGC 4621 is less than 0.5 mJy (Wrobel & Heeschen 1991) and NGC 4697 is less than 0.6 mJy (Birkinshaw & Davies 1985). From VLA data at 8.5 GHz and 10'' resolution, NGC 4621 has a candidate LLAGN that is unresolved and has a low-resolution flux density of  $0.153 \pm 0.014$  mJy (Wrobel & Herrnstein 2000). From VLA data at 8.5 GHz and about 3'' resolution, Krajinovic & Jaffe (2002) reported an upper limit for NGC 4697; but the sensitivity values claimed were not plausible given the exposure time so the VLA archival data were analyzed following the strategies outlined in § 3 and leading to a  $4\sigma$  upper limit of 0.164 mJy for these low-resolution data.

### 2.2. Chandra

X-ray data for the galaxies were retrieved from the *Chandra* archives. These galaxies were observed with the ACIS-S3 back-illuminated CCD chip. The data were reprocessed and then analyzed with the CIAO version 3.2 software package. Background levels were low and stable. The UT observation date and net exposure times appear in Table 2. Corrections were made for known aspect offsets<sup>5</sup>.

Figures 1 and 2 show the resulting images in the full (0.5-8 keV), soft (0.5-2 keV) and hard (2-8 keV) energy ranges. Several X-ray sources are seen in the central regions of each galaxy. This work focuses on the nearest and brightest X-ray sources to the NED/2MASS centroid positions marked in Figures 1 and 2. For those

X-ray sources, the WAVDETECT tool was used to measure their positions in the full energy range; the parameters used in the detection procedure are given in Terashima & Wilson (2003). The X-ray positions of these candidate LLAGNs are given in Table 2 along with the diameter of the position error circle, 1.2'' at the 90% confidence limit<sup>6</sup>. These X-ray positions are also marked in Figures 1 and 2.

Spectra were extracted from circular regions centered at the X-ray positions of the candidate LLAGNs. Extraction radii of 2.5 pixels (1.2'') and 3 pixels (1.5'') were used for NGC 4621 and NGC 4697, respectively, to maximize the signal-to-noise ratio and to minimize the contribution from adjacent emission. Spectra of the background were taken from an off-nuclear region in the same field of view and subtracted from the source spectra. Each spectral bin contains 12 and 10 counts for NGC 4621 and NGC 4697, respectively. Thus a Gaussian approximation of a Poisson distribution is not appropriate and a chi-squared method cannot be used for parameter estimation. Instead, the  $C$  statistic, a likelihood defined by using a Poisson distribution, was employed (Cash 1979). Spectral fits were performed by using XSPEC version 11.3. The spectra were fitted with a power-law model modified by the total absorption along the line of sight, thus including contributions both from the Galaxy and intrinsic to the elliptical galaxies. The best-fit parameters and errors appear in Table 1. Quoted errors are at the 90% confidence level for one parameter of interest. Table 1 also gives the  $C$  statistic per number of spectral bins, an indicator of the quality of the fit. The fitted absorption columns are consistent with the Galactic values of 2.2 and  $2.1 \times 10^{20}$  cm<sup>-2</sup> for NGC 4621 and NGC 4697, respectively (Dickey & Lockman 1990). The spectra and best-fit models are shown in Figure 3.

In addition to the candidate LLAGNs, Figures 1 and 2 show several faint X-ray sources as well as hints of extended soft X-ray emission. To provide further information about the extended emission and the population of discrete sources in each galaxy, adaptively-smoothed images were made over the central 3' in the soft (0.5-2 keV) energy band. These images appear in Figure 4.

## 3. NEW DATA

Under proposal code AW671, the VLA was used in the A configuration to observe NGC 4621 at 8.5 GHz using phase calibrator J1254+1141 and NGC 4697 at 8.5 GHz using phase calibrator J1246-0730. Phase calibrator positions were taken from the Goddard VLBI global solution 2004 f,<sup>7</sup> and had one-dimensional errors at  $1\sigma$  better than 1 mas. The switching time between a galaxy and its phase calibrator was 460 s, while switching angles were about 3° or less. The *a priori* pointing positions for NGC 4621 and NGC 4697 were taken from Wrobel & Herrnstein (2000) and Sarazin et al. (2001), respectively. Data were acquired in dual circular polarizations with a bandwidth of 100 MHz. Observations were made assuming a coordinate equinox of 2000. The UT observation date and net exposure times appear in Table 2. Observations of 3C 286 were used to set the amplitude scale to an accuracy of about 3%. Twenty-two

<sup>4</sup> Operated by the National Radio Astronomy Observatory, which is a facility of the National Science Foundation, operated under cooperative agreement by Associated Universities, Inc.

<sup>5</sup> [http://cxc.harvard.edu/cal/ASPECT/fix\\_offset/fix\\_offset.cgi](http://cxc.harvard.edu/cal/ASPECT/fix_offset/fix_offset.cgi)

<sup>6</sup> <http://cxc.harvard.edu/cal/ASPECT/celmon>

<sup>7</sup> [http://gemini.gsfc.nasa.gov/solutions/2004f\\_astro/](http://gemini.gsfc.nasa.gov/solutions/2004f_astro/)

of 27 antennas provided data of acceptable quality, with most of the data loss attributable to EVLA retrofitting activities. The data were calibrated using the 2006 December 31 release of the NRAO AIPS software. No self-calibrations were performed. No polarization calibration was performed, as only upper limits on the galaxies' linear polarization percentages were sought.

The AIPS task `imgr` was used to form and deconvolve images of the Stokes  $I$  emission at 8.5 GHz from each galaxy. The images, made with natural weighting to obtain the lowest  $1\sigma$  noise levels, appear in Figures 1 and 2. Each galaxy image was searched within the NED/2MASS error circle for emission above  $4\sigma$ , leading to the detection of an unresolved source, with diameter less than  $0.3''$ . Quadratic fits in the image plane yielded the peak flux densities appearing in Table 1, along with their errors that are quadratic sums of the 3% scale error and  $\sigma$ . Those fits also yielded the radio positions listed in Table 2 along with their 90% position-errors obtained from the quadratic sum of a term due to the signal-to-noise ratio of the detection and a term due to the phase-referencing strategies, estimated to be  $\sigma = 0.1''$  (the errors in the phase calibrator positions were negligible). The radio positions are marked in Figures 1 and 2. `imgr` was also used to form naturally-weighted images of Stokes  $Q$  and  $U$  from each galaxy. Those images showed the same values for  $\sigma$  as their Stokes  $I$  counterparts but led to no detections.

#### 4. IMPLICATIONS FROM THE ASTROMETRY

Each of these nearby elliptical galaxies have been detected in the new high-resolution VLA images shown in Figures 1 and 2. Each high-resolution radio detection occurs within the error circle for the galaxy centroid position. Thus each galaxy harbors a bona fide LLAGN that has been localized at radio frequencies with sub-arcsecond accuracy. The position of the high-resolution radio detection of NGC 4621 is consistent with the previous radio detection at low resolution, which was taken to mark a candidate LLAGN. NGC 4697 has no prior radio detection and thus no prior radio astrometry.

Candidate LLAGNs have been identified in the high-resolution *Chandra* images derived from archival data and shown in Figures 1 and 2. The position of the candidate LLAGN in NGC 4697 is consistent with that reported for Source 1 by Sarazin et al. (2001). NGC 4621 has no prior X-ray astrometry. Formally, the X-ray positions of these two candidate LLAGNs are consistent with the centroid positions of the host galaxies from NED/2MASS.

For NGC 4621 and NGC 4697, the separations between the high-resolution radio and X-ray positions are about  $0.6''$  and  $0.5''$ , respectively. The quadratic sum of the  $1\sigma$  error in the radio astrometry ( $0.1''$ ) and the X-ray astrometry ( $0.3''$ ) is about  $0.32''$ , leading to normalized separations of  $0.6''/0.32'' \sim 1.9$  for NGC 4621 and  $0.5''/0.32'' \sim 1.6$  for NGC 4697. These normalized separations are less than 3, implying valid radio/X-ray matches for both galaxies (Condon & Dressel 1978).

Thus the X-ray positions of the candidate LLAGNs are consistent with the positions of their high-resolution radio detections, meaning that NGC 4621 and NGC 4697 each host a bona fide LLAGN that has been identified at both X-ray and radio frequencies. The X-ray sources are

therefore referred to as LLAGNs in Table 2 and Figure 3.

### 5. IMPLICATIONS FROM THE PHOTOMETRY

#### 5.1. X-Ray Properties

From Table 1, the X-ray luminosities of the LLAGNs in NGC 4621 and NGC 4697 conform to the luminosity limit of  $L(2-10\text{ keV}) < 10^{42}$  ergs  $\text{s}^{-1}$  for the X-ray definition of a LLAGN (Terashima & Wilson 2003). The tabulated photon indices conform to the range of values, 1.6 to 2.0, shown by other LLAGNs (Terashima & Wilson 2003). The X-ray photometry given in Table 1 for the LLAGN in NGC 4697 is consistent with that reported for Source 1 by Sarazin et al. (2001) and Soria et al. (2006a). Also, the latter study analyses data from 2000 and from 2003-2004, and finds no evidence for significant spectral or luminosity changes over that long term.

NGC 4621 and NGC 4697 each host a supermassive black hole with  $M_{\bullet} > 10^8 M_{\odot}$ , for which the characteristic Eddington luminosity is  $L(\text{Edd}) > 10^{46}$  ergs  $\text{s}^{-1}$  (Table 1). In stark contrast, the observed X-ray luminosities are lower by about 9 orders of magnitude, and using them as a proxy for a bolometric luminosity, the black holes energizing the LLAGNs in NGC 4621 and NGC 4697 are found to have Eddington ratios  $L(2-10\text{ keV})/L(\text{Edd}) \sim 10^{-9}$  (Table 1). Such ratios are very sub-Eddington.

#### 5.2. Radio and Circumnuclear Properties

For the LLAGN in NGC 4621, the flux density at 8.5 GHz measured at a resolution of about  $10''$  (880 pc) in 1999 (§ 2) is higher than that measured at a resolution of  $0.3''$  (26 pc) in 2006 (Table 1). This difference could arise from time variability and/or from source resolution effects in NGC 4621. Variability on typical timescales of a few days has been established at 8.5 GHz for other LLAGNs (Anderson & Ulvestad 2005). A difference due to source resolution effects in NGC 4621 could be linked to jet-like emission driven by the LLAGN, or to the stellar substructures on scales of about  $2''$  (180 pc) that are traced either kinematically (Wernli et al. 2002) or photometrically (Krajinovic & Jaffe 2004). But a stellar origin seems unlikely for two reasons. First, the Palomar spectrum shows only an old stellar population (Ho et al. 2003a). Second, if the flux-density difference arises from star formation, then converting it to 1.4 GHz with a spectral index of  $-0.7$  implies a star-formation rate of about  $0.0045 M_{\odot} \text{ yr}^{-1}$  (Yun et al. 2001), for which the  $\text{H}\alpha$  luminosity (Kennicutt 1998) would be about 6 times higher than its observed upper limit (Ho et al. 2003a). The left panel of Figure 4 shows a population of discrete X-ray sources, presumably low-mass X-ray binaries. There also appears to be soft X-ray emission on a scale of a few kiloparsecs, but this faint emission may partly arise from blends of discrete sources and, based on Figure 4, it will be difficult to characterize the diffuse gas potentially available for accretion onto the black hole.

For the LLAGN in NGC 4697, the flux-density upper limit at 8.5 GHz measured at a resolution of about  $3''$  (170 pc) in 2000 (§ 2) is consistent with the detection at a resolution of  $0.3''$  (17 pc) in 2006 (Table 1). NGC 4697 has a probable stellar cluster centered on a dusty disk with a diameter of  $7''$  (400 pc) (Soria et al. 2006a). The right panel of Figure 4 shows evidence for soft X-ray emission on a scale of a few kiloparsecs, consistent with prior reports by Sarazin et al. (2001) and

Soria et al. (2006a). This diffuse emission is characterized by a “temperature” of 0.33 keV and a central gas density of  $0.02 \text{ cm}^{-3}$ ; this gas, as well as the gas released by the stellar populations, is potentially available for accretion within the black hole’s sphere of influence of diameter  $0.76''$  (44 pc) (Soria et al. 2006a,b). The right panel of Figure 4 also shows a population of discrete X-ray sources, identified as low-mass X-ray binaries in prior studies (Sarazin et al. 2001; Soria et al. 2006a).

### 5.3. Radio Loudness

The study of Palomar LLAGNs using *Chandra*, the VLA, and the VLBA found that the majority are radio loud, defined as  $\log R_X = \log \nu L_\nu(5 \text{ GHz})/L(2 - 10 \text{ keV}) = -4.5$  or higher (Terashima & Wilson 2003). That study involved radio sources with flat or inverted spectra, so the cited definition applies equally well at 8.5 GHz as at 5 GHz. As shown in Table 1, the emission from the quiescent black holes in NGC 4621 and NGC 4697 is radio-loud, with  $\log R_X = \log \nu L_\nu(8.5 \text{ GHz})/L(2 - 10 \text{ keV}) \sim -2$ . Since radio continuum emission is outflow-dominated (Nagar et al. 2005), this suggests the presence of a radio outflow on scales less than 26 pc in NGC 4621 and less than 17 pc in NGC 4697 (§ 3). Barring strong projection effects, the length scale of the 8.5-GHz emission from NGC 4697 would place it inside the black hole’s sphere of influence (Soria et al. 2006a,b).

### 5.4. The Radio–X-ray–Mass Relation

A relationship among radio luminosity, X-ray luminosity and black-hole mass was discovered by Merloni et al. (2003) and Falcke et al. (2004) for accretion-powered systems. For LLAGNs in particular this so-called fundamental plane (FP) relation supports the idea that they are massive analogs of black hole X-ray binaries in the low/hard state, with Eddington ratios of about  $10^{-5}$  to  $10^{-3}$ . Within this framework, general models for the central engine of a LLAGN (e.g., Yuan et al. 2000b) contain (1) a cool, optically-thick, geometrically-thin accretion disk with a truncated inner radius; (2) a hot, radiatively-inefficient accretion flow (RIAF) interior to the truncation radius; and (3) an outflow/jet. Application of such models to black hole X-ray binaries in the low/hard state can lead to strong tests involving both spectral and timing properties. For example, the coupled accretion-jet model of Yuan et al. (2005) was successfully tested in this way. The outflow emission in that model was treated using the internal-shock picture widely applied to gamma-ray bursts. For the low/hard binary tested, the outflow dominated the radio and infrared emission, the thin disk dominated the UV emission, the hot RIAF dominated the X-ray emission, and all three components contributed to the optical emission. In addition, the Yuan et al. (2005) model was shown to be consistent with the FP relation (Yuan & Cui 2005). Cast in the notation of Table 1, the FP relation of Merloni et al. (2003) is  $\log \nu L_\nu(5 \text{ GHz}) = 0.60 \log L(2 - 10 \text{ keV}) + 0.78 \log(M_\bullet/M_\odot) + 7.33$ , with a scatter of  $\sigma = 0.88$ . Given this large scatter, the relation can be used to estimate the 8.5-GHz luminosity  $\nu L_\nu(8.5 \text{ GHz})$  expected for NGC 4621 and NGC 4697 from their black hole masses and X-ray luminosities (Table 1). These FP-based predictions are  $\nu L_\nu(8.5 \text{ GHz}) \sim 4.0 \times 10^{36} \text{ ergs s}^{-1}$  for

NGC 4621 and  $\nu L_\nu(8.5 \text{ GHz}) \sim 1.4 \times 10^{36} \text{ ergs s}^{-1}$  for NGC 4697. Although these predictions have uncertainties of almost an order of magnitude, both are about that amount below the galaxies’ observed  $\nu L_\nu(8.5 \text{ GHz})$  listed in Table 1.

The black holes in NGC 4621 and NGC 4697 are very sub-Eddington, featuring ratios of about  $10^{-9}$  (Table 1). For other similar systems, departures from the FP relation have been suggested (e.g., Fender et al. 2003; Markoff 2005). Within the context of the coupled accretion-jet model (Yuan et al. 2005) described above, the very sub-Eddington ratios for NGC 4621 and NGC 4697 place them in the model’s so-called quiescent regime (Yuan & Cui 2005). Moreover, the black holes in NGC 4621 and NGC 4697 are able to generate radio emission which, as argued in the previous subsection, is plausibly jet-like. Thus the “if the jet persists” caveat for the quiescent regime seems to be fulfilled, and motivates application of the radio–X-ray–mass relation for the quiescent regime (Yuan & Cui 2005). Cast in the notation of Table 1, that quiescent relation is  $\log \nu L_\nu(8.5 \text{ GHz}) = 1.23 \log L(2 - 10 \text{ keV}) + 0.25 \log(M_\bullet/M_\odot) - 13.45$ , and the black hole masses and X-ray luminosities in Table 1 yield the predicted radio luminosities  $\nu L_\nu(8.5 \text{ GHz})$  appearing in Table 1. Those predicted radio luminosities agree, to within a factor of a few, with the observed radio luminosities, also listed in Table 1. Significantly, the radio–X-ray–mass relation for the quiescent regime invokes X-ray emission from the outflow rather than from an accretion flow. Also, Yuan & Cui (2005) note that their index for the quiescent relation, 1.23, is in general agreement with earlier pure outflow models (e.g., Heinz 2004).

In the coupled accretion-jet model (Yuan et al. 2005), the outflow/jet generates synchrotron emission which is optically-thick near 8.5 GHz and optically-thin at hard X-rays. In the model’s quiescent regime (Yuan & Cui 2005), the emission from the outflow dominates over that from any thin disk and any hot RIAF. Specifically, the spectral energy distribution of the outflow curves smoothly across the electromagnetic spectrum, and photon indices near 2, like those observed (Table 1), seem achievable in the hard X-rays (Yuan & Cui 2005). For comparison, Comptonization in a RIAF acts as a natural thermostat, limiting the electron temperature to about 100 keV. At the very low accretion rates associated with the quiescent regime, any feeble RIAF would generate 100-keV bremsstrahlung emission which has a photon index of 1.3 in the *Chandra* band. Such an index is not consistent with the measured value for NGC 4621 but is just consistent with the measured value for NGC 4697 (Table 1). In the latter case, some bremsstrahlung contribution to the 2-10 keV luminosity could account for the model’s slight overprediction of the 8.5-GHz luminosity.

## 6. SUMMARY AND FUTURE DIRECTIONS

Analysis of *Chandra* data and VLA data shows that the nearby elliptical galaxies NGC 4621 and NGC 4697 each contain a low-luminosity active galactic nucleus (LLAGN), identified as a faint, hard X-ray source that is astrometrically coincident with a faint 8.5-GHz source. These frequency regions benefit from high contrast against the stellar emission, little or no obscuration, and subarcsecond angular resolution and astrometry.

The massive black holes energizing these LLAGNs have Eddington ratios  $L(2 - 10 \text{ keV})/L(\text{Edd}) \sim 10^{-9}$ , placing them in the quiescent regime. These quiescent black holes are radio-loud emitters, suggesting the presence of a radio outflow. Application of the radio–X-ray–mass relation from Yuan & Cui for quiescent black holes predicts the observed radio luminosities  $\nu L_\nu(8.5 \text{ GHz})$  to within a factor of a few. Importantly, that relation invokes X-ray emission from the outflow rather than from an accretion flow. In the radio and X-ray regions, the faint, but detectable, emission from these two massive black holes is therefore consistent with being outflow-dominated.

Clearly, the spectral energy distributions of the LLAGNs in NGC 4621 and NGC 4697 need to be measured across the electromagnetic spectrum. Deep VLA observations at frequencies of 1-50 GHz would test the Yuan & Cui prediction of optically-thick emission from

the LLAGNs, as well as enable searches for faint, jet-like structures adjacent to the LLAGNs. Also, short-term variability on timescales of a few days has been found at 8.5 GHz for other LLAGNs (Anderson & Ulvestad 2005). For each of the LLAGNs in NGC 4621 and NGC 4697, evidence for short-term, correlated variability between the radio source and the X-ray source would strengthen the case for their common, outflow origin. Finally, more cases like NGC 4621 and NGC 4697 are needed to better define the population of quiescent LLAGNs, and the improved sensitivity of the Expanded VLA will help enormously on this front (Ulvestad et al. 2006).

We acknowledge the valuable feedback from an anonymous referee.

*Facilities: Chandra, VLA.*

#### REFERENCES

- Anderson, J. M., & Ulvestad, J. S. 2005, *ApJ*, 627, 674  
 Bietenholz, M. F., Bartel, N., & Rupen, M. P. 2000, *ApJ*, 532, 895  
 Birkinshaw, M., & Davies, R. L. 1985, *ApJ*, 291, 32  
 Cash, W. 1979, *ApJ*, 228, 939  
 Condon, J. J., & Dressel, L. L. 1978, *ApJ*, 221, 456  
 Condon, J. J., Cotton, W. D., Greisen, E. W., Yin, Q. F., Perley, R. A., Taylor, G. B., & Broderick, J. J. 1998, *AJ*, 115, 1693  
 Dickey, J. M., & Lockman, F. J. 1990, *ARA&A*, 28, 215  
 Falcke, H., & Biermann, P. L. 1999, *A&A*, 342, 49  
 Falcke, H., & Markoff, S. 2000, *A&A*, 362, 113  
 Falcke, H., Koerding, E., & Markoff, S. 2004, *A&A*, 414, 895  
 Fender, R. P., Gallo, E., & Jonker, P. G. 2003, *MNRAS*, 343, L99  
 Heinz, S. 2004, *MNRAS*, 355, 835  
 Ho, L. C. 2004, *Coevolution of Black Holes and Galaxies*, ed. L. C. Ho (Cambridge: CUP), 292  
 Ho, L. C., Filippenko, A. V., & Sargent, W. L. W. 1997, *ApJS*, 112, 315  
 Ho, L. C., et al. 2001, *ApJ*, 549, L51  
 Ho, L. C., Filippenko, A. V., & Sargent, W. L. W. 2003a, *ApJ*, 583, 159  
 Ho, L. C., Terashima, Y., & Ulvestad, J. S. 2003b, *ApJ*, 589, 783  
 Kennicutt, R. C., Jr. 1998, *ARA&A*, 36, 189  
 Kormendy, J. 2004, *Coevolution of Black Holes and Galaxies*, ed. L. C. Ho (Cambridge: CUP), 1  
 Krajnovic, D., & Jaffe, W. 2002, *A&A*, 390, 423  
 Krajnovic, D., & Jaffe, W. 2004, *A&A*, 428, 877  
 Livio, M., Ogilvie, G. I., & Pringle, J. E. 1999, *ApJ*, 512, 100  
 Markoff, S. 2005, *ApJ*, 618, L103  
 Meier, D. L. 2001, *ApJ*, 548, L9  
 Merloni, A., Heinz, S., & Di Matteo, T. 2003, *MNRAS*, 345, 1057  
 Nagar, N. M., Falcke, H., & Wilson, A. S. 2005, *A&A*, 435, 521  
 Narayan, R., Yi, I., Mahadevan, R. 1995, *Nature*, 374, 623  
 Pellegrini, S. 2005, *ApJ*, 624, 155  
 Pinkney, J., et al. 2005, *ApJ*, 596, 903  
 Ravindranath, S., Ho, L. C., & Filippenko, A. V. 2002, *ApJ*, 566, 801  
 Sarazin, C. L., Irwin, J. A., & Bregman, J. M. 2001, *ApJ*, 556, 533  
 Soria, R., et al. 2006a, *ApJ*, 640, 126  
 Soria, R., et al. 2006b, *ApJ*, 640, 143  
 Terashima, Y., & Wilson, A. S. 2003, *ApJ*, 583, 145  
 Terashima, Y., Ho, L. C., & Ulvestad, J. S. 2005, *The Interplay among Black Holes, Stars and ISM in Galactic Nuclei*, IAUS 222, eds. T. Storchi-Bergmann et al. (Cambridge: CUP), 61  
 Thompson, A. R., Clark, B. G., Wade, C. M., Napier, P. J., 1980, *ApJS*, 44, 151  
 Tremaine, S., et al. 2002, *ApJ*, 574, 740  
 Ulvestad, J. S., Perley, R. A., McKinnon, M. M., Owen, F. N., Dewdney, P. E., & Rodriguez, L. F. 2006, *BAAS*, 38, 135  
 Wernli, F., Emsellem, E., & Copin, Y. *A&A*, 396, 73  
 White, R. L., Becker, R. H., Helfand, D. J., & Gregg, M. D. 1997, *ApJ*, 475, 479  
 Wrobel, J. M., & Heeschen, D. S. 1991, *AJ*, 101, 148  
 Wrobel, J. M., & Herrnstein, J. R. 2000, *ApJ*, 533, L111  
 Yuan, F., Markoff, S., & Falcke, H. 2000a, *A&A*, 383, 854  
 Yuan, F., Markoff, S., Falcke, H., & Biermann, P. L. 2000b, *A&A*, 391, 139  
 Yuan, F., Cui, W., & Narayan, R. 2005, *ApJ*, 620, 905  
 Yuan, F. & Cui, W. 2005, *ApJ*, 629, 408  
 Yun, M. S., Reddy, N. A., & Condon, J. J. 2001, *ApJ*, 554, 803

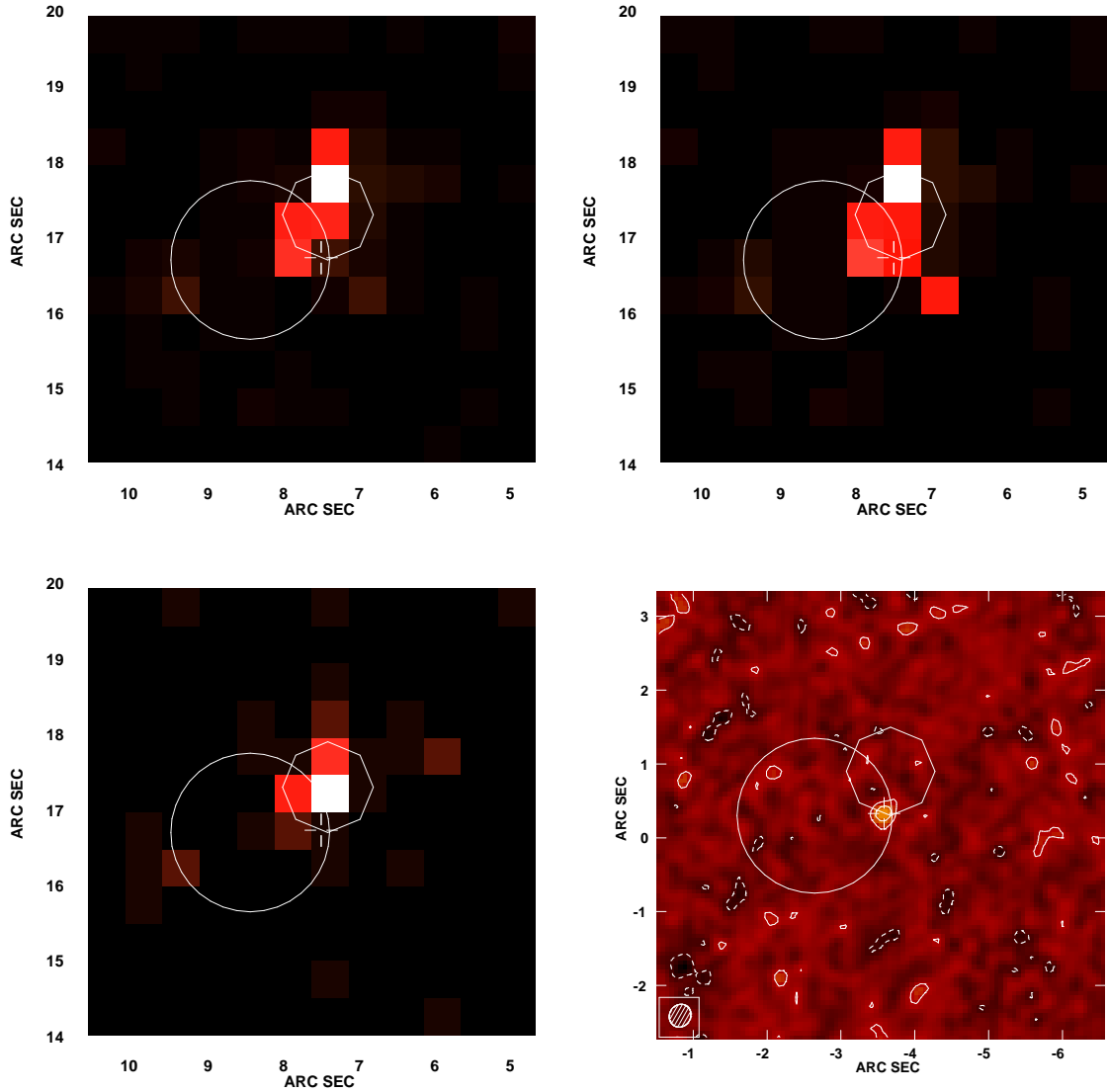


FIG. 1.— Images of the central  $6''$  (530 pc) of NGC 4621. The symbols mark positions and their errors at the 90% confidence level. The NED/2MASS position of the galaxy centroid is marked with a circle, while the octagon marks the *Chandra* position of the nearest and brightest source to the NED/2MASS position. The high-resolution VLA position from this work is marked with a cross with a gap. *Top left*: *Chandra* image at 0.5-8 keV with a peak of 16 counts. *Top right*: *Chandra* image at 0.5-2 keV with a peak of 12 counts. *Bottom left*: *Chandra* image at 2-8 keV with a peak of 5 counts. In the *Chandra* images, the coordinate labels are relative to the aim point (to convey that astrometric distortions should be negligible) and the logarithmic color scale spans zero to the peak. *Bottom right*: VLA image of Stokes  $I$  emission at a frequency of 8.460 GHz. Coordinate labels are relative to the pointing position. Natural weighting was used, giving an rms noise of  $0.018 \text{ mJy beam}^{-1}$  ( $1 \sigma$ ) and beam dimensions at FWHM of  $0.32'' \times 0.29''$  with elongation  $\text{PA} = -30^\circ$  (hatched ellipse). Contours are at -6, -4, -2, 2, 4, and 6 times  $1 \sigma$ . Negative contours are dashed and positive ones are solid. Linear color scale spans  $-0.06 \text{ mJy beam}^{-1}$  to  $0.20 \text{ mJy beam}^{-1}$ .

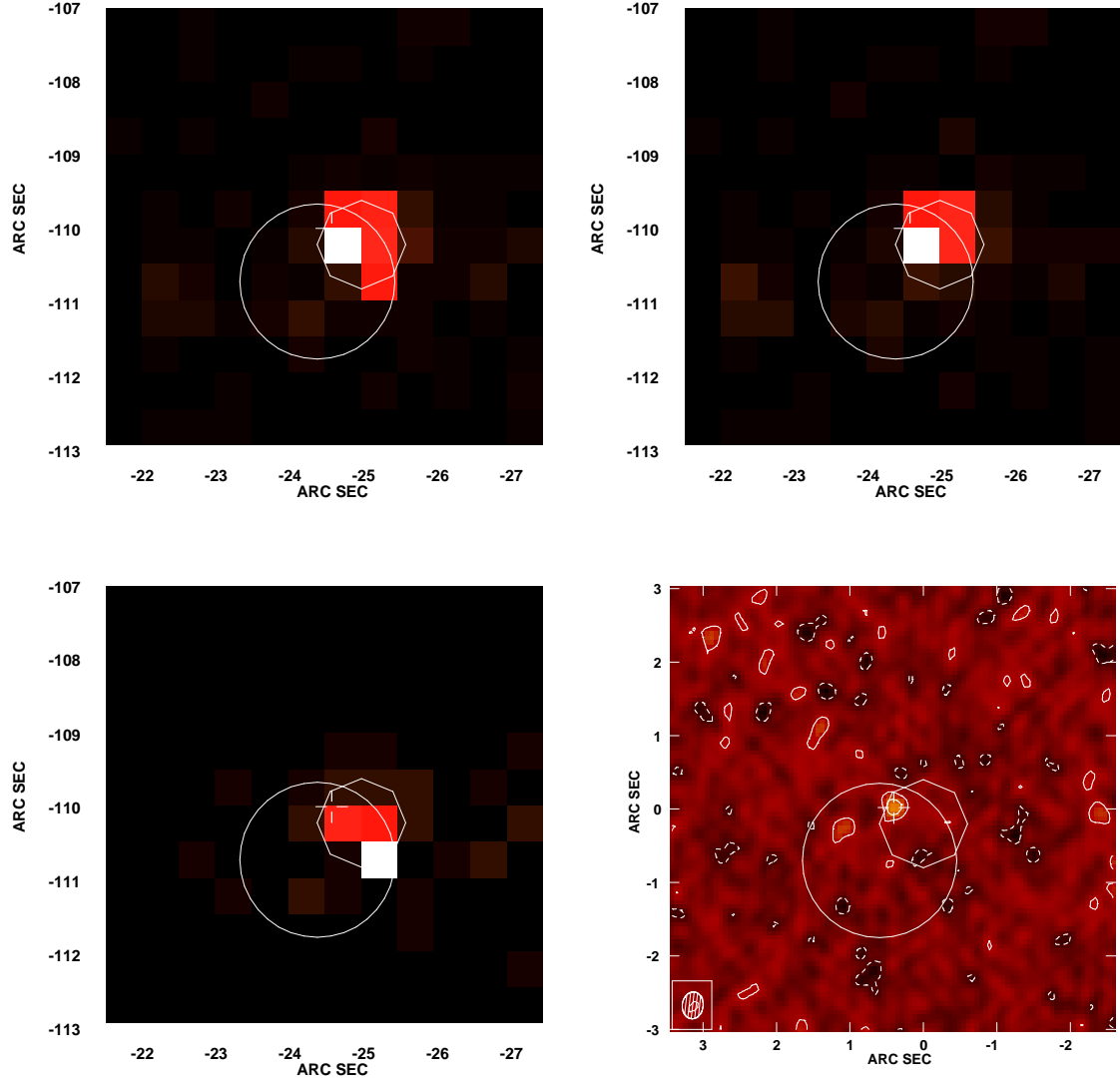


FIG. 2.— Images of the central  $6''$  ( $340$  pc) of NGC 4697. In the *Chandra* images the peaks are 18 counts (*top left*), 14 counts (*top right*) and 6 counts (*bottom left*). In the VLA image the noise is  $0.017$  mJy beam<sup>-1</sup> ( $1 \sigma$ ) and the beam dimensions at FWHM are  $0.37'' \times 0.28''$  with elongation PA =  $-6^\circ$  (*bottom right*). Otherwise as for Figure 1.

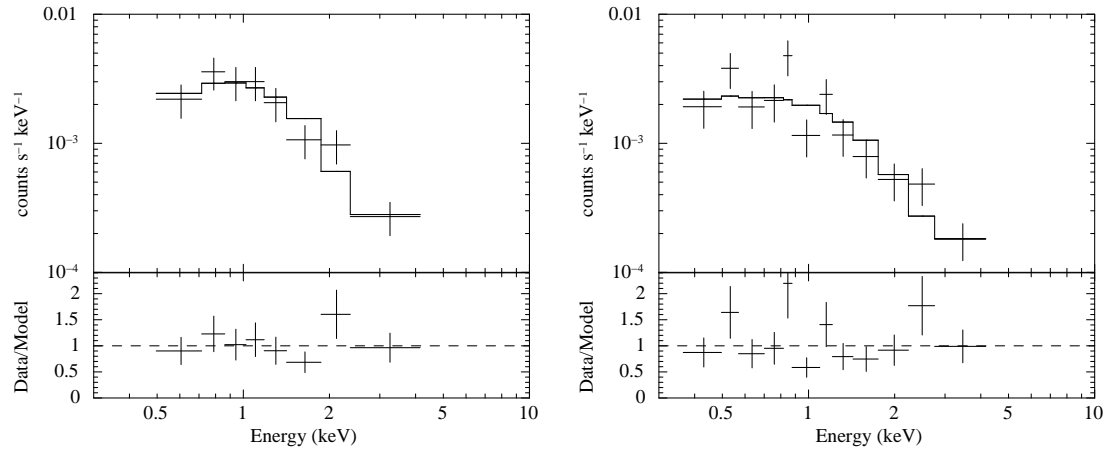


FIG. 3.— *Chandra* spectra of the LLAGNs in NGC 4621 (*left*) and NGC 4697 (*right*). Each top panel shows crosses for the data and a histogram for the model. Each bottom panel shows the ratio of the data to the model, a preferred diagnostic when the  $C$ -statistic is employed.



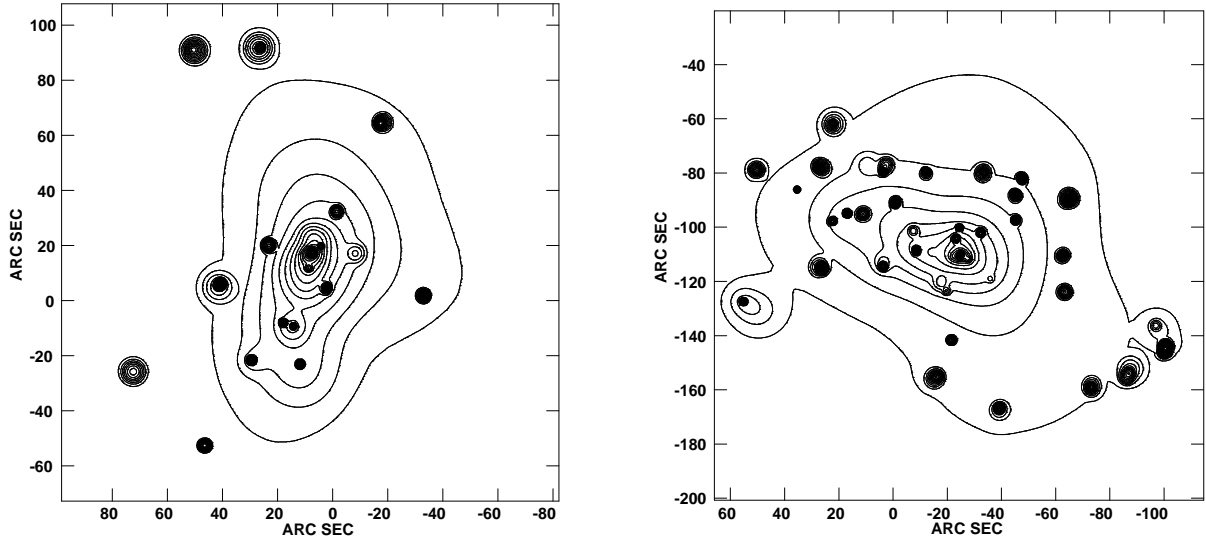


FIG. 4.— Adaptively-smoothed *Chandra* images at 0.5-2 keV with contours spaced by factors of the square root of 2. *Left*: Central 3' (16 kpc) of NGC 4621. Lowest contour is 0.007 and peak is 6.8, in units of smoothed counts. *Right*: Central 3' (10 kpc) of NGC 4697. Lowest contour is 0.02 and peak is 39, in units of smoothed counts.

TABLE 1  
PARAMETERS OF THE LLAGNS

Parameter	NGC 4621	Ref.	NGC 4697	Ref.
$D$ (Mpc)	18.2	1	11.7	2
$s$ (pc arcsec $^{-1}$ )	88	1	57	2
$M_{\bullet}$ ( $10^8 M_{\odot}$ )	2.7	3	1.7	2
$L(Edd)$ ( $10^{46}$ ergs s $^{-1}$ )	3.5	3	2.2	2
$N_{\text{H}}$ ( $10^{20}$ cm $^{-2}$ )	<18.	4	<8.4	4
$\Gamma$	$1.8^{+0.8}_{-0.3}$	4	$1.6^{+0.5}_{-0.3}$	4
$C$ statistic per number of spectral bins	5/8	4	17/12	4
$F(2-10\text{ keV})$ ( $10^{-14}$ ergs s $^{-1}$ cm $^{-2}$ )	$2.1^{+1.2}_{-1.0}$	4	$1.7\pm 0.7$	4
$L(2-10\text{ keV})$ ( $10^{37}$ ergs s $^{-1}$ )	6.6	4	2.2	4
$L(2-10\text{ keV})/L(Edd)$ ( $10^{-9}$ )	1.9	4	1.0	4
$S(8.5\text{ GHz})$ (mJy)	$0.098\pm 0.018$	4	$0.092\pm 0.017$	4
Observed $\nu L_{\nu}(8.5\text{ GHz})$ ( $10^{35}$ ergs s $^{-1}$ )	3.3	4	1.3	4
$\log R_X = \log \nu L_{\nu}(8.5\text{ GHz})/L(2-10\text{ keV})$	-2.3	4	-2.2	4
Predicted $\nu L_{\nu}(8.5\text{ GHz})$ ( $10^{35}$ ergs s $^{-1}$ )	1.5	5	3.5	5

REFERENCES. — (1) Ravindranath et al. 2002; (2) Pellegrini 2005; (3) Tremaine et al. 2002; (4) this work; (5) Yuan & Cui 2005

NOTE. — Row (1): Surface-brightness-fluctuation distance. Row (2): Scale. Row (3): Mass of black hole. Row (4): Eddington luminosity of black hole. Row (5): Galactic plus intrinsic column density. Row (6): Photon index. Row (7):  $C$  statistic (Cash 1979). Row (8): 2-10 keV flux. Row (9): 2-10 keV luminosity. Row (10): Eddington ratio. Row (11): 8.5 GHz flux density. Row (12): Observed radio luminosity. Row (13): Radio loudness. Row (14): Predicted radio luminosity.

TABLE 2  
ASTROMETRY OF THE GALAXY COMPONENTS

Galaxy (1)	Component (2)	Region (3)	R.A. (J2000) (4)	Decl. (J2000) (5)	Error ( $''$ ) (6)	Date (7)	Exposure (s) (8)	Ref. (9)
NGC 4621 ...	Galaxy centroid	K	12 42 02.32	11 38 48.9	2.1	...	...	1
	LLAGN	X	12 42 02.25	11 38 49.5	1.2	2001 Aug 1	24837	2
	LLAGN	R	12 42 02.256	11 38 48.93	0.43	2006 Apr 21	6630	2
NGC 4697 ...	Galaxy centroid	K	12 48 35.91	-05 48 03.1	2.1	...	...	1
	LLAGN	X	12 48 35.87	-05 48 02.6	1.2	2000 Jan 15-16	39260	2
	LLAGN	R	12 48 35.897	-05 48 02.38	0.43	2006 Apr 21	6060	2

REFERENCES. — (1) NED/2MASS; (2) this work.

NOTE. — Col. (1): Galaxy name. Col. (2): Nuclear component. Col. (3): Frequency region coded as K for near-infrared, R for radio at 8.5 GHz and X for X-ray. Cols. (4) and (5): Component position. Units of right ascension are hours, minutes, and seconds, and units of declination are degrees, arcminutes, and arcseconds. Col. (6): Diameter of error circle at 90% confidence level. Col. (7): UT observation date. Col. (8): Exposure time. Col. (9): Reference.